Composites: Part A 190 (2025) 108617

Contents lists available at ScienceDirect

Composites Part A

journal homepage: www.elsevier.com/locate/compositesa

Enhanced electromechanical performance of structural supercapacitor composites with high loading of graphene nanoplatelet at the fibre/matrix interface

Jayani Anurangi [a,b,c], Janitha Jeewantha [a,b], Madhubhashitha Herath [a], Dona T.L. Galhena [d], Jayantha Epaarachchi [a,b,*]

[a] School of Engineering, Faculty of Health Engineering and Sciences, University of Southern Queensland, Toowoomba, Australia
[b] Centre for Future Materials, Institute for Advanced Engineering and Space Sciences, University of Southern Queensland, Toowoomba, Australia
[c] Department of Biosystems Technology, Faculty of Technological Studies, Uva Wellassa University of Sri Lanka, Passara Road, Badulla, Sri Lanka
[d] Churchill College, University of Cambridge, UK

HIGHLIGHTS

- GNP coating changes surface wettability which improves electrochemical performance.
- GNP coating at the fibre/matrix interface boosts electromechanical performance.
- Enhanced thermal properties of the structural supercapacitor composites.
- GNP-coated structural supercapacitor composites perform well under tensile loading.
- In-situ electrochemical testing under mechanical loading shows stable performance.

GRAPHICAL ABSTRACT

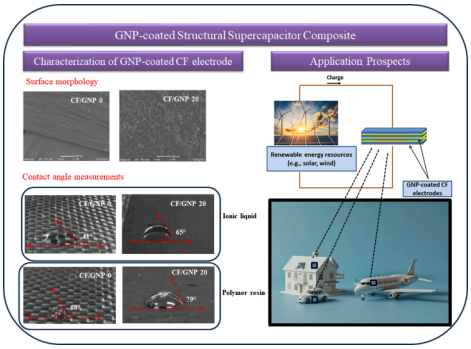

ARTICLE INFO

Keywords:
Structural supercapacitor composite
Carbon fibre
Fibre/matrix interface
Energy storage
Graphene nanoplatelet

ABSTRACT

A structural supercapacitor composite (SSC) is a multifunctional device that can perform load-bearing operations simultaneously while storing electrical energy. In this study, the impact of high loading graphene nanoplatelet (GNP) on carbon fibre (CF) electrodes on the electromechanical performance of SSC was studied. A stable GNP coating at the fibre/matrix interface with poly-tetrafluoroethylene (PTFE) binder was obtained. GNP loading enhances the surface wettability of CF electrodes with the structural electrolyte, improving the electrochemical performance. The developed SSC demonstrated a specific capacitance of 123.5 mF g^{-1}, with a 77 % improvement. In addition, after GNP loading, the tensile strength increased to 254.4 MPa, the modulus reached to 18.0 GPa, and the flexural strength improved to 48.9 MPa. In-situ mechano-electrochemical tests of SSCs showed over 60 % capacitance retention with no significant difference until mechanical failure occurred. These findings provide essential knowledge for further improvements of next-generation multifunctional energy storage composites.

* Corresponding author.
E-mail address: Jayantha.Epaarachchi@unisq.edu.au (J. Epaarachchi).

https://doi.org/10.1016/j.compositesa.2024.108617
Received 10 September 2024; Received in revised form 20 November 2024; Accepted 24 November 2024
Available online 30 November 2024

1. Introduction

Currently, many composite material researchers are developing multifunctional polymer composites that offer additional capabilities beyond their primary functions, such as specific strength, lightweight and durability. These added functionalities include energy storage and harvesting, electromagnetic interference shielding, and radar absorption. Incorporating several functions into one material is an ideal solution to increase the overall efficiency and usability of the material [1,2]. Among the multifunctional materials, structural energy storage composites have attracted considerable attention due to their potential to significantly reduce the weight and volume of devices, which currently rely on conventional energy storage devices and load-bearing structural materials [3,4]. Herein, the structural supercapacitor composite (SSC) has gained much attention in the industry, as this device can be readily integrated into structural components such vehicle body parts or buildings, providing mechanical support while simultaneously storing energy [5,6].

On the other hand, ever-growing environmental consciousness, increasing fuel costs, and continuous depletion of oil reserves have escalated the demand for renewable and sustainable energy sources [7–9]. Using renewable energy resources constantly urges people to explore advanced energy storage technologies [10]. In this context, the SSCs provide an excellent opportunity to integrate energy generation directly into structural components, thereby enhancing the overall efficiency of the entire energy system. Carbon fibre reinforced polymer composites (CFRC), widely used in many industries, has emerged as a promising candidate for developing SSC [4,11].

CFRC has been extensively used in automobiles [12], structural parts such as wind turbines [13,14], buildings, and civil constructions for decades owing to its exceptional mechanical and physical properties [15,16]. There is a growing interest in broadening the range of CFRC applications by developing multifunctional materials [1,17,18]. Therefore, much research aims to develop SSC using CFRC [19–22]. However, the energy storage capability of CFRC is still at its inception since pristine carbon fibre (CF) cannot deliver the expected electrochemical performances because of chemical inertness and limited active-surface area [23,24]. Though highly challenging, surface activation of CF fabric was very effective in tackling this issue [25]. Different methods, such as activation, heteroatom doping, and surface deposition, are available for enhancing the surface area of carbon fibres [26]. Among these methods, the deposition of electrochemically active nanomaterials on CF surfaces and modifying the fibre/matrix interface have improved the electrochemical properties substantially [4]. Carbon nanomaterials, such as activated carbon [27], CNT [28,29], carbon aerogel [30], graphene nanoflakes [24], graphene aerogel (GA) [31], and graphene nanoplatelets (GNP) [32,33], can be coated on the surface of CF to enhance the electrochemical performance.

Recent studies reveal that GNP is one of the best candidates for enhancing the electrochemical properties of CF-based SSCs. GNP can enhance supercapacitor performance by elevating energy density, power density, and cycle life [34]. Meanwhile, the engineered fibre/matrix interface in the composites can improve the mechanical properties by effectively transferring the load between the matrix and reinforcement [35,36]. Thus, the surface treatment of CF using GNP coating can enhance the mechanical properties by strengthening the interphase region and limiting the movement of the epoxy [37]. In addition, it is believed that the fibre surface characteristics, such as porosity [23] and roughness [2], are changed after GNP coating, which directly affects the electromechanical properties of the SSC. Therefore, developing GNP-modified CF electrodes is a plausible solution for acquiring high electromechanical properties.

However, CF electrodes coated with active materials face challenges in maintaining structural integrity, as the active material may detach following electrochemical cycling [21]. Therefore, improving the interface stability of the electrode following such modification is crucial for enhancing the performance of structural supercapacitors. In this regard, various researchers have used different binders (e.g., PVDF, PVA) to ensure the adhesion of GNP particles onto the electrodes [33]. These binders promote the mechanical integrity and durability of CF electrodes. However, researchers have underestimated the role of binders during the past few years and made fewer efforts to boost the capacitive behaviour via exploring and developing novel binders.

A Binder is a critical component of an electrode, which acts as a dispersion agent to connect the active materials and ensure adherence to the CF current collector [38]. It modifies the wettability and facilitates ion transport at the electrode/electrolyte interface. Therefore, selecting a proper binder for the adhesion of GNP on CF is vital for optimizing the electromechanical properties.

Zhu and co-workers [39] demonstrated that poly-(tetrafluoroethylene) (PTFE) is one of the best binders for supercapacitors assessed from the comprehensive electrochemical performances such as specific capacitance, stability, rate capability with significant capacitance retention over 80 %. PTFE enhances adhesive strength between the active material particles and the current collector, helping to prevent the active material from leaching during charging and discharging cycles [34]. However, no significant study has explored the effect of GNP coating with PTFE binder on the electromechanical performance of structural supercapacitors. Therefore, this research systematically investigated the outcome of GNP coating with PTFE binder on multifunction properties, focusing mainly on electrical and mechanical properties.

In this study, the GNP loading on CF was varied to investigate its influence on the electromechanical properties of SSC. The results revealed that the optimized CF/GNP 20 SSC achieved a specific capacitance of 123.5 mF g^{-1} and an energy density of 38.6 mWh kg^{-1}, with exceptional cycling stability exceeding 5000 cycles. CF/GNP 10 SSC shows the highest mechanical properties, with a tensile strength of 254.4 MPa and a flexural strength of 48.9 MPa, demonstrating its capacity to withstand significant external mechanical load. In addition, the in-situ mechano-electrochemical tests demonstrate that the electrochemical behaviour of the developed SSC remains stable even under mechanical load.

2. Experimentation

2.1. Materials and chemicals

This research utilized pristine woven carbon fibre HexForce^{TM} 282 (3 K wrap/fill yarn, 33MSI), a bi-axial 0/90 fabric (200 gsm, 2/2 Twill), with a ± 45 fibre orientation serving as the electrodes. E-glass fibre fabric (120 gsm, plain weave) was employed as the separator of the structural supercapacitor. GNP (750 m^2/g, Sigma Aldrich) was used here for surface modification of CF electrode. The PTFE (60 wt% dispersion in H2O, Sigma Aldrich) acted as a binder when making GNP slurry with IPA solvent (98 %, FG, Sigma Aldrich). Triton X-100 (Sigma Aldrich) was used as the surfactant for better dispersion of GNP.

The resin matrix was Bisphenol A epoxy resin Araldite GY 191 with Triethylenetetramine hardener (TETA, 97 %, purchased from Sigma Aldrich). 1-Ethyl-3-methylimidazolium bis(trifluoro methylsulfonyl) imide (EMITFSI, 98 %, purchased from Sigma Aldrich) was used as the ionic liquid. Bis(trifluoromethane) sulfonamide lithium salt (LiTFSI, purchased from Sigma Aldrich), propylene carbonate (PC, 99.7 %, purchased from Sigma Aldrich), and industrial-grade TiO_2 (99 %, 20–40 nm, XFNANO China) were mixed with the ionic liquid of EMITFSI for preparing liquid electrolyte. All chemical reagents were used without further purification.

2.2. Preparation of the GNP slurry

The GNP slurry was prepared by mixing 3 wt% GNP, 0.6 wt% PTFE and 0.2 wt% Triton-X in IPA solvent. The PTFE binder fixed the GNP on

the surface of the CF fabric, and Triton X-100 acted as the surfactant. The slurry was ultrasonicated using a tip sonicator (Sonoplus ultrasonic homogenizers, power 200 W) for 30 min (50 % amplitude, on 5 s and off 5 s).

2.3. Preparation of GNP-coated CF electrodes

Initially, CF fabrics were cleaned with acetone to remove sizing agents and dried in an oven. Then, the prepared GNP slurry was sprayed onto the CF surface, layer by layer, using a manual spray gun at a 2–3 bar pressure range while maintaining a 10–15 cm distance between the fabric and the spray gun. After applying each GNP layer, the CF fabric was dried in an oven for 5–10 min before applying the next layer. This process was repeated for both sides of the fabric, which was then oven-dried at 100 °C for 3 hrs to ensure complete evaporation of all solvents. The active GNP mass loading on the CF electrode was determined from the mass increment of the CF/GNP fabrics relative to the pristine CF fabrics (Eq. S1). The GNP loadings approximately varied from 0 wt% (CF/GNP 0), 5 wt% (CF/GNP 5), 7.5 wt% (CF/GNP 7.5), 10 wt% (CF/GNP 10) and 20 wt% (CF/GNP 20).

2.4. Preparation of structural electrolyte

Following the process suggested in previous works [40,41], 11.8 g EMIMTFSI, 0.1 g PC, and 1 g LiTFSI were mixed using magnetic stirring for 30 min to obtain the liquid electrolyte (LE). The prepared LE was

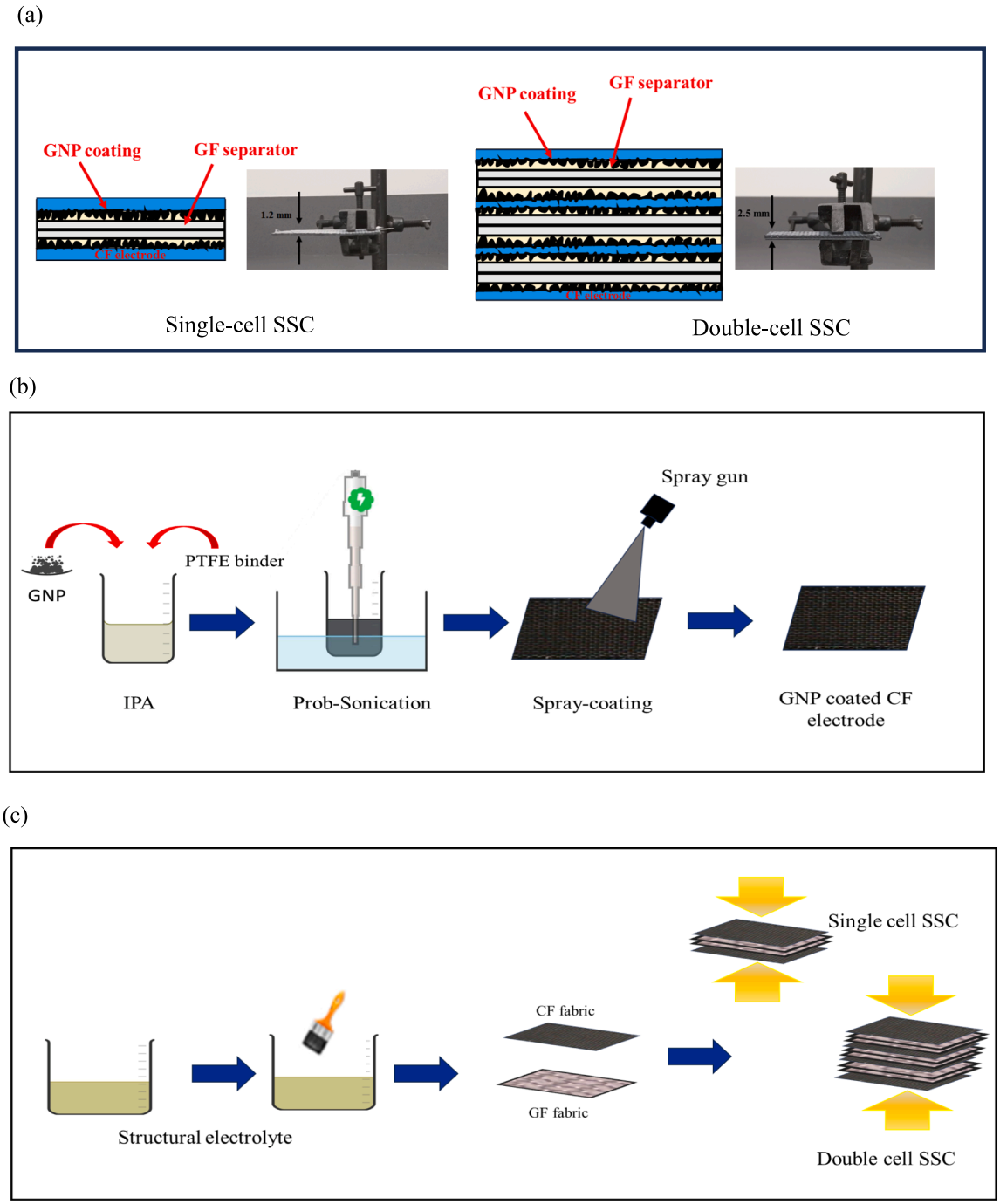

Fig. 1. A schematic illustration of (a) single-cell and double-cell configurations, (b) GNP electrode preparation, (c) SSC fabrication.

mixed with 3.65 g DGEBA for 20 min until it became a homogeneous solution. Then added 0.5 g of TiO_2 and stirred for another 30 min. Finally, TETA hardener was added to the mixture in a mass ratio of DGEBA to TETA 7.81: 1, and the mixture was stirred for five minutes at room temperature to form the structural electrolyte (SE) solution. The prepared SE solution contains 75 % LE and 25 % structural resin matrix.

2.5. Manufacturing of structural supercapacitor composite

The GNP-coated CF fabric was cut into a rectangular of 50 mm × 80 mm, and a copper sheet was attached to the surface to provide electrical contacts for subsequent electrochemical testing. Then, single-cell and double-cell structural supercapacitors were fabricated with each type of GNP-coated CF electrode. The lay-up configuration of the single-cell supercapacitor was CF-GF-GF-CF, and the double-cell configuration was CF-GF-GF-CF-GF-GF-CF-GF-GF-CF, as shown in Fig. 1(a). The effective GNP-coated surface area of SSC was 50 mm × 50 mm (as shown in figure S1(a-c)). The structural electrolyte mixture was evenly coated on CF electrodes and GF separators in a fully open environment and mechanically pressed for curing at room temperature (25 °C) for 48 h. Then, it was heated for three hours in an oven at 65 °C for the post-curing process. The GNP uncoated part of the CF electrodes was not impregnated with the structural electrolyte to connect them to the potentiostat.

Fig. 1(b) and 1(c) schematically illustrate the GNP coating and structural supercapacitor fabrication. The thicknesses of single-cell and the double-cell SSC were measured at approximately 1.2 mm and 2.5 mm, respectively.

2.6. Investigation of surface properties of CF electrodes

2.6.1. Surface morphology

The surface morphology of CF electrodes after GNP coating and the surface morphology of cured structural electrolyte in bulk, prior to reinforcements, were characterized using scanning electron microscopy (SEM, JEOL JCM-6000).

2.6.2. Investigation of surface wetting behaviour

The effect of increasing GNP loading on the hydrophilicity of the CF fabric surface was investigated using contact angle measurements in relation to two solutions (i.e., IL or polymer resin). Therefore, the contact angels of pristine (CF/GNP 0) and GNP-coated CF electrodes (CF/GNP 5, CF/GNP 7.5, CF/GNP 10, and CF/GNP 20) with IL and polymer resin were studied according to ASTM D7334 [42]. Here, a 20 μL droplet of polymer resin or IL was dropped on different types of CF electrodes, and then the images of contact angles of the droplets were captured by a camera at different elapsed times. Finally, the contact angles of droplets were analysed using ImageJ software to study the wettability change.

2.6.3. Investigation of thermal properties of SSC

The thermogravimetric analysis (TGA) and dynamic mechanical analysis (DMA) were carried out for double-cell configuration to determine the thermal property changes due to GNP coating on CF electrodes. TGA was performed using a TA Instruments Discovery SDT 650. The temperature was raised from room temperature to 600 °C at a rate of 10 °C min^{-1} under a continuous flow of N_2 gas. The viscoelastic properties of the structural supercapacitors were analysed using the DMA test conducted with a TA instrument HR-2 Discovery Hybrid Rheometer in a dual cantilever fixture. The specimen dimensions were 45 mm × 8 mm, and the test was conducted over a temperature window of 20 °C to 150 °C at a rate of 5 °C/min, with a displacement of 25 μm applied at a frequency of 1 Hz.

2.7. Mechanical testing of SSC

The mechanical properties of developed GNP-coated SSCs (double-cell configuration) were evaluated by tensile and bending tests according to the ASTM D3039 [43] and ASTM D790 [44] standards [45], respectively. All specimens were prepared using a water jet cutter in accordance with the relevant standards. A slight reduction in structural properties is anticipated due to the exposure of the IL to water during the cutting process. Structural properties were evaluated using an MTS 10 kN (Insight Electromechanical) uni-axial testing machine. To enhance the grip of the machine clamps, glass fibre composite end tabs with 50 mm × 50 mm dimensions were bonded to the tensile test specimens. An extensometer with a gauge length of 25 mm (figure S2(a)) was used, and Young's modulus was calculated by analysing the trendline on the stress–strain curve, using strain data recorded by the extensometer. Five measurements were taken for each test to ensure accuracy and reliability of the results. The fibre weight fractions of the five types of structural supercapacitors (CF/GNP 0, CF/GNP 5, CF/GNP 7.5, CF/GNP 10, and CF/GNP 20) were measured according to ASTM D3171 [46].

2.8. Electrochemical testing of SSC

All electrochemical measurements were taken using an *Autolab* electrochemical interface instrument (PGSTAT 302 N) in the two-electrode configuration. The electrochemical performance was expressed with respect to the total device mass which includes the CF electrodes with copper sheets, GF separators and structural electrolyte. Cyclic voltammetry (CV) tests at different scan rates in a voltage window of 0 V to 1.5 V for single-cell and double-cell SSCs were conducted for qualitative study. The electrochemical impedance spectroscopy (EIS) was performed for single-cell structural supercapacitors at an amplitude of 100 mV in a frequency range of 0.01 Hz–100 kHz (30 measuring points) to obtain the Nyquist plot. The variation of specific capacitance and energy density were evaluated with galvanostatic charge–discharge (GCD) tests at 0.2 mA g^{-1} current density according to the GNP loading on CF fabric at room temperature (25 °C). The fabricated double-cell SSCs were also cycled 5000 times through CV at 10 mVs^{-1} for the life-time measurement.

2.9. In-situ mechano-electrochemical test

The in-situ mechano-electrochemical tests were performed in this study to characterize the multifunctionality of SSC. Here, three-point bending tests investigated the electrochemical properties of SSC under different static loads. The electrochemical performance test is measured when the external load is applied to the CF/GNP 10 double-cell SSCs. As shown in Fig. 2, a force was applied at the midpoint of the specimen, inducing different bending deformations (from 0 mm to 10 mm) until reaching mechanical failure. Subsequently, CV measurements at a scan rate of 5 mVs^{-1} were conducted for each deflection (δ). In addition, the electrochemical performance was recorded by conducting a CV test at 5 mVs^{-1} scan rate with respect to the three different bending and releasing cycles (50, 100, and 150) at five deflections (0 mm, 1 mm, 2 mm, 3 mm, and 5 mm).

3. Results and discussion

The mechanical properties of SSC were evaluated using tensile and flexural test results, while electrochemical performance was investigated based on CV, GCD and EIS test results. The results of in-situ mechano-electrochemical performance evaluated the multifunctionality of the developed SSC. Finally, a proof-of-concept was conducted by lighting up a commercial LED to demonstrate the device's suitability for practical applications.

3.1. Microstructural analysis of CF electrode

Fig. 3(a)-3(d) present the scanning electron microscopy (SEM) images of CF surface with varying GNP loadings. A relatively uniform,

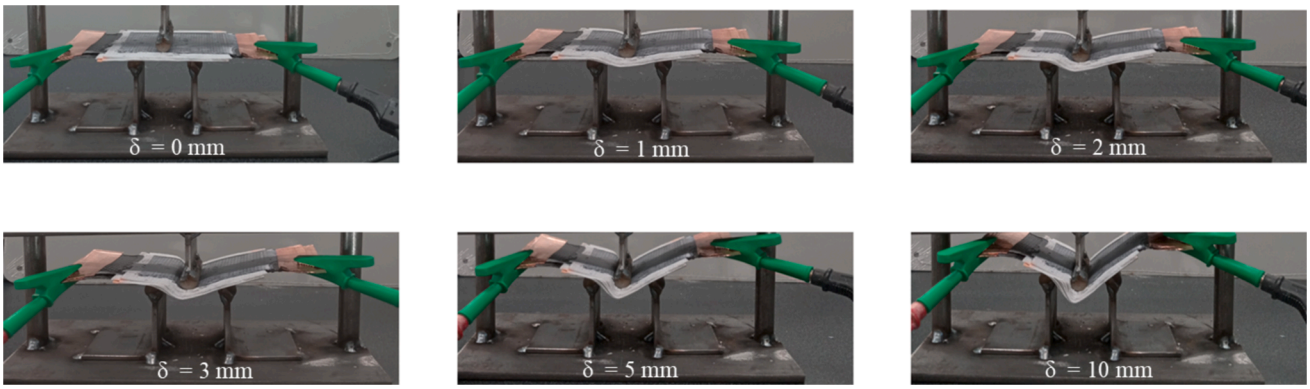

Fig. 2. In-situ mechano-electrochemical test under different bending deformation.

thick layer of GNP coating was observed on the fibre surfaces. Increased GNP loading formed a continuous graphene layer on top of the CF surface without enclosing individual fibres. The crimps and gaps between carbon fibres and within the fibre bundles were fully occupied with nanostructured GNP (Fig. 3(d) and 3(e)), providing more surface area to store ions at the electrode/electrolyte interface.

Fig. 3(f) shows the microstructure of the structural electrolyte analysed by SEM. Before SEM observation, ionic liquid in structural electrolytes was removed by acetone extraction to avoid image distortion. As shown in Fig. 3(f), the ionic liquid creates a separated phase inside the structural resin matrix and forms a bi-continuous structure, providing channels for ion movement inside the matrix. However, due to the change of wettability on the surfaces of CFs, particularly after GNP coating, the microstructure of the structural electrolyte changes at the surface, as explained in the next section (3.2).

3.2. Change of CF surface wettability

Contact angle measurements provided detailed information about the surface wettability in relation to the solution. Fig. 4 shows the contact angles of the pristine and GNP-modified CF electrodes with the polymer resin (Fig. 4(a)) and ionic liquid (Fig. 4(b)) which were used for preparing the structural electrolyte. The contact angles for all samples decreased to zero after some time due to capillary force, but the rate of decrease depends on the GNP loading.

First, the wetting behaviour of pristine CF with polymer resin and IL was studied. The initial contact angles of pristine CF electrodes are 41^0 with polymer resin and 68^0 with ionic liquid, as reported in Table 1. The contact angles drop to below 20^0 within milli seconds, supporting the argument that both the polymer resin and ionic liquid in the bi-continuous structural electrolyte equally wet the pristine CF electrode surface.

Next, the change of contact angles of CF electrodes with ionic liquid and polymer resin was tested after GNP coatings. The contact angles of

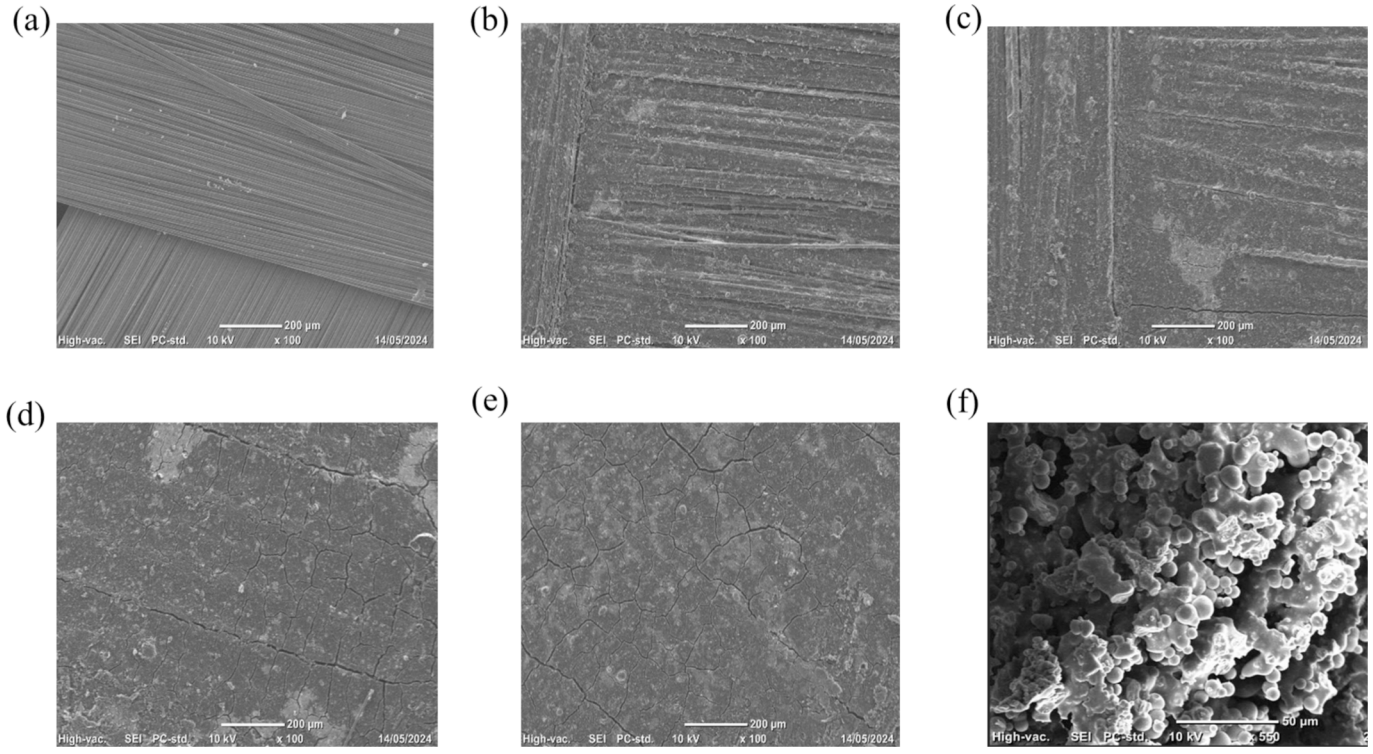

Fig. 3. SEM images. (a) CF/GNP 0, (b) CF/GNP 5, (c) CF/GNP 7.5, (d) CF/GNP 10, (e) CF/GNP 20, and (f) Structural electrolyte (after ionic liquid extraction by acetone).

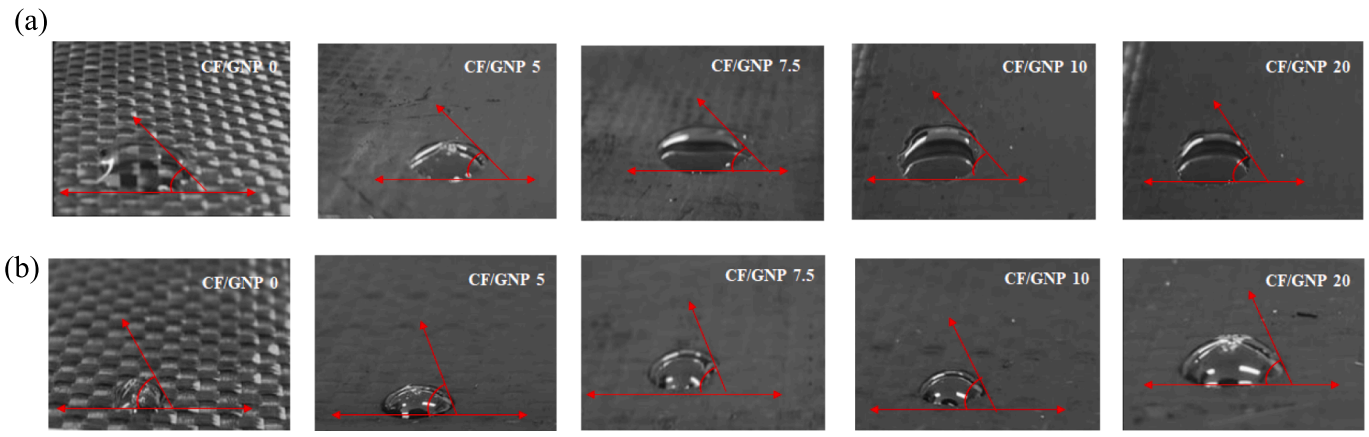

Fig. 4. The initial contact angles with (a) IL and (b) polymer resin with increasing GNP loading on CF electrodes.

Table 1
Contact angle of CF electrode with polymer resin and liquid electrolyte.

Type of CF electrode	IL	Polymer resin
CF/GNP 0	41	68
CF/GNP 5	58	65
CF/GNP 7.5	59	66
CF/GNP 10	62	72
CF/GNP 20	65	79

GNP-modified CF electrodes with ionic liquid were consistently lower than those of polymer resins after GNP coating. Further, the elapsed time for completely wetting the GNP-modified surface (contact angle $< 20°$) by ionic liquid slightly increased with GNP loading, i.e., less than 3 min, for all GNP-modified CF surfaces. However, the elapsed time for completely wetting the GNP-modified surface (contact angle $< 20°$) by polymer resin significantly increased with GNP loading; it took over 10 min to wet the GNP-modified CF surfaces completely. Therefore, the wettability of CF electrodes with the structural electrolyte has improved due to GNP coating. Hence, it is possible to conclude that ionic liquid wets the GNP-modified CF surfaces more effectively than polymer resins. Consequently, GNP coating on CF electrodes enhances the contact between the electrode and the IL compared to polymer resin. This reduces the area covered by polymer resin while increasing the area of direct contact between the electrodes and the ionic liquid.

3.3. *Effect of GNP loading on thermal properties*

The thermal stability of SSCs with increased GNP loading, from 0 wt % to 20 wt%, was assessed by conducting a TGA test under a continuous flow of N_2 gas. Fig. 5(a) shows the weight change as a function of the increasing temperature. Decomposition has two stages. The first region occurs in the temperature range between 275 °C and 325 °C, followed by the second region with a temperature range of 325 °C to 475 °C. The first degradation of the SSCs with increased GNP loading has been shifted slightly to higher temperatures compared to the SSC without GNP coating (Fig. 5(a) inset). This specifies the positive effect of GNP on the thermal stability of the nanocomposites. Both GNP and CF are degraded during the second region, while the glass fibre remains as the residue when the temperature exceeds 500 °C. In summary, the CF/GNP 20 has increased the first degradation temperature by 7 % compared to the controlled SSC due to the addition of GNP, confirming the enhancement effect on the thermal stability of the composite.

The DMA test was conducted to study the change of viscoelastic properties over a range of temperatures in relation to GNP loading. Fig. 5 (b) illustrates the storage moduli versus temperature curves for SSCs

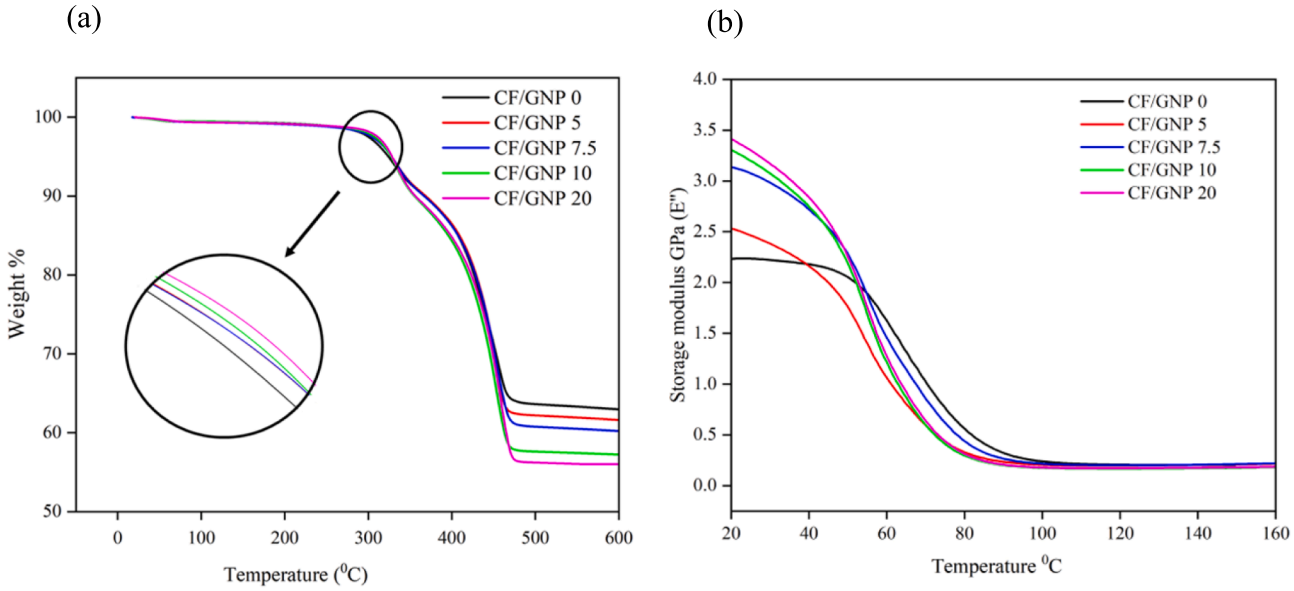

Fig. 5. (a) TGA and (b) Storage modulus curves of double-cell SSC with increasing GNP loading on CF electrodes.

with increased GNP loading. A significant increase in the storage moduli (E") from 2.2 GPa to 3.5 GPa occurred when GNP loading was increased to 20 wt% at room temperature.

3.4. Effect of GNP loading on mechanical properties

The mechanical performance of the structural supercapacitor device is of utmost importance for real-world utilization. The fibre weight fractions of the five types of structural supercapacitors (CF/GNP 0, CF/GNP 5, CF/GNP 7.5, CF/GNP 10, and CF/GNP 20) were calculated as 51.6 %, 51.4, 52.6 % 51.8 %, and 53.1 % for CF/GNP 0, CF/GNP 5, CF/GNP 7.5, CF/GNP 10, and CF/GNP 20, respectively. Since there is no significant difference in weight ratios of fibre to resin, the reinforcement does not have a substantial impact on the variations of mechanical properties among the five structural supercapacitor composites.

The tensile and flexural behaviour of the developed double-cell SSCs were studied for each types of SSCs. Fig. 6(a) and 6(b) present stress–-strain curves. The ultimate tensile strength and flexural strength values (Table 2) were calculated based on Eq. S2 and Eq. S3. The Young's modulus was evaluated from the trendline of the stress–strain curve, based on the extensometer readings. To understand the failure mechanisms in tensile testing, the failure modes of the tested specimens were analysed. All SSC specimens exhibited delamination failure during tensile testing, in accordance with the tensile failure guidelines outlined in ASTM D3039. The failure code defined in the standard characterises the failure type (1st character), failure area (2nd character) and failure location (3rd char acter). Accordingly, failure mode of the SSCs can be categorised as "DGM (Edge delamination-Gage-Middle)".

Additionally, the tensile data of specimens shows a distinct change in tensile properties after coating GNP on the CF surface, and tensile strengths of SSCs were significantly increased after GNP coating on CF surface. Control specimens produced without GNP coating showed the lowest tensile strength and Young's modulus with values of 109.5 MPa and 9.7 GPa, respectively.

GNP coating improved the fibre/matrix interface, significantly enhancing the tensile properties such as Young's modulus and ultimate tensile strength. However, tensile properties barely changed with different GNP loading, and no significant changes were observed with varying GNP loading. Maximum modulus of 18.8 GPa was reported at 5 % GNP loading, which shows a twofold increase compared to the control specimen. Ultimate tensile properties slightly increased from 5 wt% to 10 wt% GNP. At 10 wt% GNP loading, tensile strength was 254.4 MPa. When GNP loading reached 20 wt%, tensile strength showed a small reduction, with a value of 227.6 MPa. All GNP-coated SSCs failed due to delamination (figure S2) with high strains during the tensile test, consistent with findings reported in the existing literature [47,48]. Notably, the low ultimate tensile strength and modulus values, as well as the high strain values, are attributed to the use of 0/90 woven CF fabric and the off-axis tensile loading at a 45° angle.

The flexural performance is evaluated to study the structural behaviour of the SSCs when subjected to bending forces (Fig. 6(b)). Applying a bending load provides critical insights into the flexural properties and overall performance of the materials under realistic loading conditions. While the GNP coating on the CF surface significantly enhances tensile strength but does not result in a significant improvement in flexural strength. The lack of enhancement of flexural strength is attributed to a reduction in interlaminar shear strength, which can lead to delamination (Figure S3). Notably, delamination occurred without complete fracture, indicating that the material maintained structural integrity and robustness despite layer separation. Therefore, it can be concluded that the developed structural supercapacitor devices have the potential to be used for energy storage applications without significantly compromising the structural integrity.

3.5. Effect of GNP loading on electrochemical properties

According to Fig. 7(a) and Table 2, the GNP coating on CF significantly improves the capacitance performance of SSC. The specific capacitance values of the structural supercapacitor based on the CV and GCD curves were calculated by applying Eq. S4 and Eq. S5, respectively. The energy density was calculated by using Eq. S6. The pristine CF-based SSC has the lowest specific capacitance due to the limited availability of the surface area for the ions to accumulate at the electrode/electrolyte interface. The highest specific capacitance (123.5 mF g^{-1}) was achieved when 20 % of GNP was loaded on the CF surface, exceeding some previously reported values in the literature as summarized by Greenhalgh et al. [22]. This provides a useful benchmark for comparing the performance of the developed SSC with other devices.

The increased specific capacitance with increasing GNP loading on CF electrodes is due to the increasing surface area, which enhances ion accumulation at the electrode/electrolyte interface. However, when increasing GNP loading, the CV curves display lilted loops, indicating high resistive behaviour due to the high resistance of the electrode/electrolyte interface. As shown in figure S4, the slopes of the loops increase with increased scan rate in each SSC type due to the insufficient time for ions to diffuse into the internal electrode pores [24]. As a result,

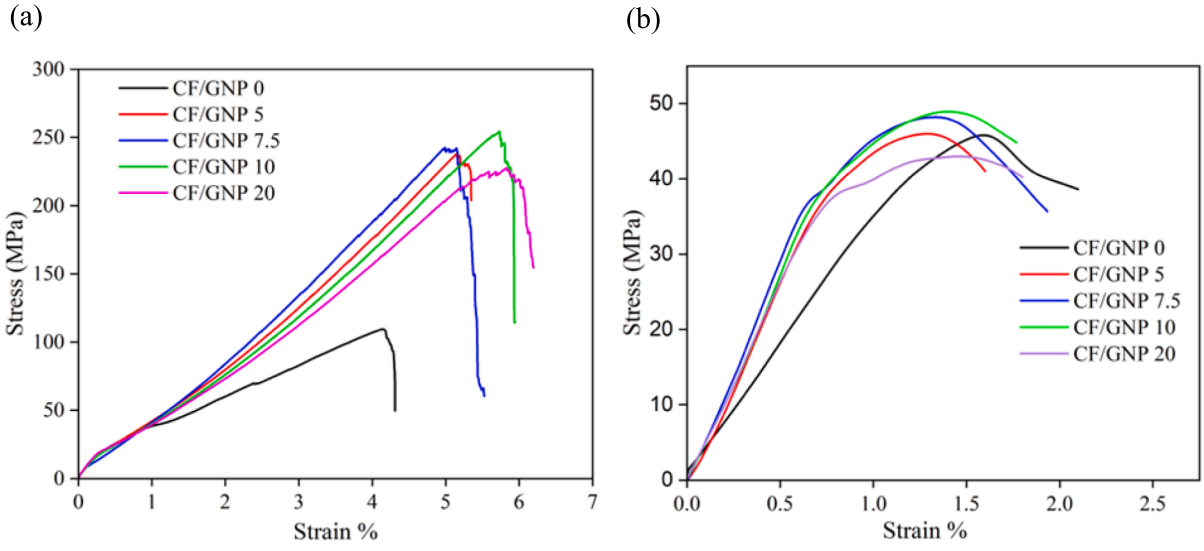

Fig. 6. (a) Tensile properties and (b) Flexural properties.

Table 2
Effect of GNP loading on mechanical and electrochemical properties of structural supercapacitors.

Sample	$C_{sp,\ CV}$ (mF g^{-1})	$C_{sp,\ GCD}$ (mF g^{-1})	E_{GCD} (mWh kg^{-1})	R_s (ESR) (Ω. cm^2)	R_p (Ω)	CPE (n)	Tensile strength (MPa)	Tensile modulus (GPa)	Flexural strength (MPa)
CF/GNP 0	2.3	1.6	0.5	1.17	62.04	0.35	109.5	9.7	45.8
CF/GNP 5	8.9	5.8	1.8	0.30	84.78	0.54	237.9	18.8	46.0
CF/GNP 7.5	13.5	25.4	7.9	0.41	95.72	0.47	242.5	18.4	48.2
CF/GNP 10	27.6	109.9	34.3	0.44	27.96	0.57	254.4	18.0	48.9
CF/GNP 20	59.2	123.5	38.6	0.16	22.27	0.32	227.6	18.0	43.0

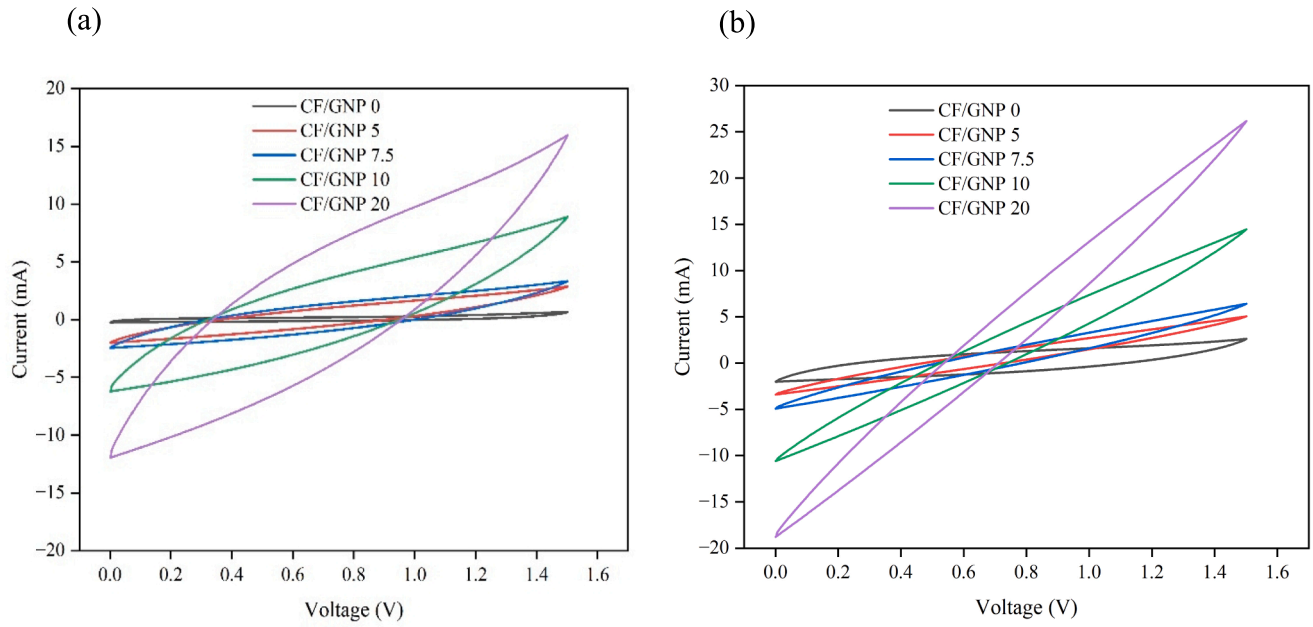

Fig. 7. Cyclic voltammetry curves of single-cell SSCs with pristine CF electrodes and GNP coated-CF electrodes with increasing loadings of GNP (a) at 5 mVs^{-1}; (b) at 10 $mVs^{-1.}$

the CF/GNP 5 and CF/GNP 7.5 SSCs exhibit low area under the CV curves compared to CF/GNP 0 SSC at high scan rates (Fig. 7(b)).

The change in surface wettability of CF electrodes with the bi-continuous structural electrolyte explains the increased specific capacitance with increased GNP loading. As described in Section 3.2, GNP loading on the CF electrode enhances the contact of the electrode with IL than polymer resin. This reduces the CF surface area covered by polymer resin and increases the area with IL being in direct contact with the electrodes, thus improving the electrochemical performance.

The EIS analysis was conducted for each type of GNP-coated SSC to evaluate the effect of GNP loading on electrochemical parameters. Fig. 8 (a) illustrates Nyquist plots for different types of SSCs. All the Nyquist plots exhibit semicircles in high-frequency regions, while linear plots in low-frequency regions. Electrical characteristics were evaluated based on the Randles electrical equivalent circuit (Fig. 8 (b)) by electrochemical circuit fit using Nova 2.1.4 software. This model consists of an equivalent series resistance (ESR), represented by Rs, in series with a parallel combination of a constant phase element represented by CPE and the parallel charge transfer resistance represented by Rp. According to the fitting parameters, the smallest semicircles of CF/GNP 10 and CF/GNP 20 SSCs are attributed to the nano-porous network structure of the GNP that improves the specific surface area of the CF electrodes and reflects a faster redox rate at the electrode/electrolyte interface. However, the CF/GNP 5 and CF/ GNP 7.5 SSCs have larger semicircles than CF/ GNP 0 SSC. This can be explained by the increase of parallel charge transfer resistance, as shown in Table 2, which is attributed to the

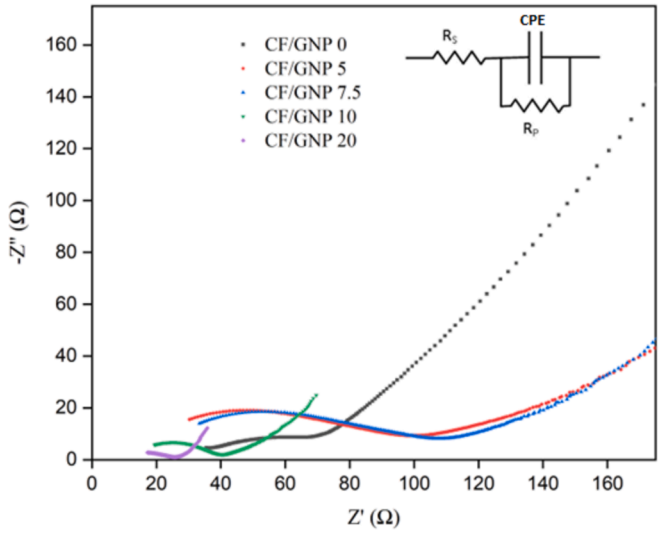

Fig. 8. (a) EIS results with Randles electrical equivalent circuit.

surface modification with GNP and PTFE binder coating at low concentrations.

The charging and discharging capacity of the double-cell SSCs were studied ((Fig. 9(a)) and presented in Table 2. The specific energy density

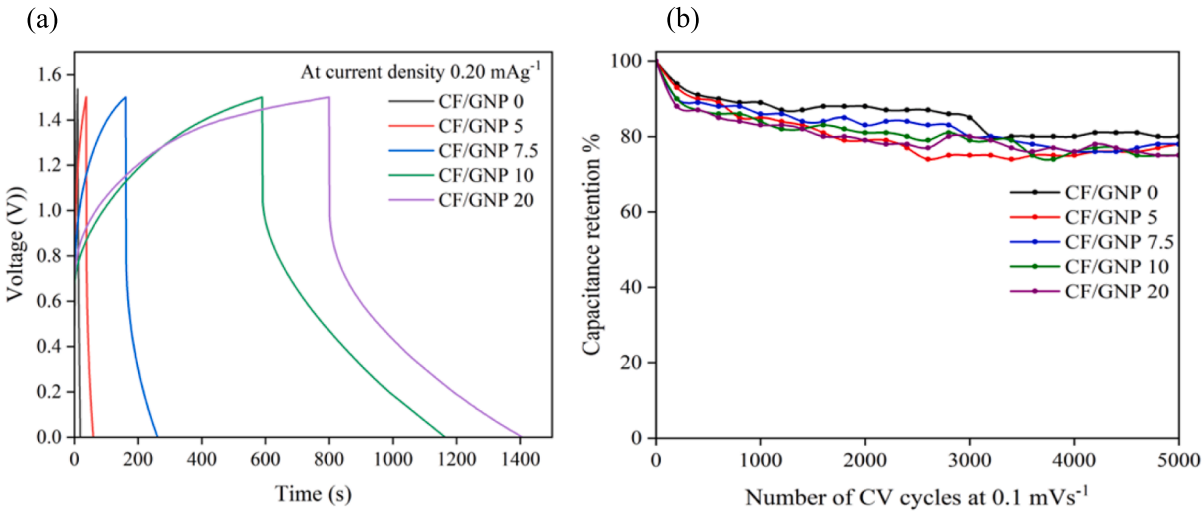

Fig. 9. (a) Charge-discharge test results and (b) Stability test results.

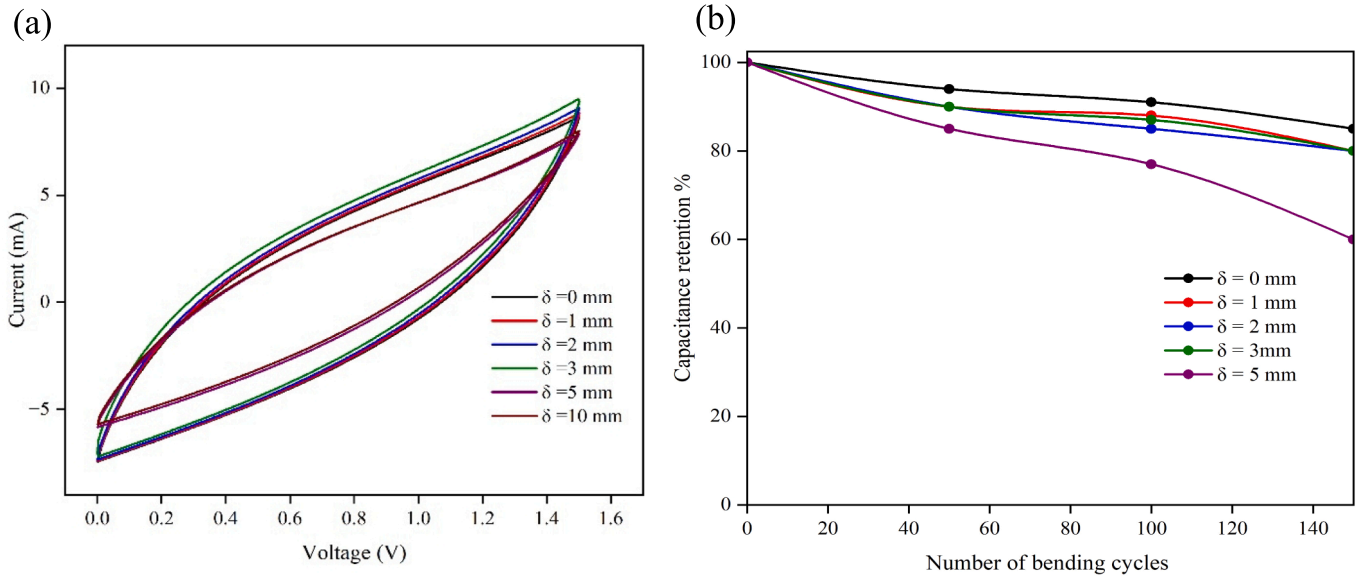

Fig. 10. (a) In-situ electromechanical performance and (b) capacitance retention after different bending cycles.

of SSC was increased to 38.6 mWh kg^{-1} with 20 wt% GNP coating. Fig. 9 (b) shows the capacitance retention after 5000 cycles. A minor variation in specific capacitance was noted after 5000 CV cycles. The stable specific capacitance values at repetitive cycles of the fabricated SSCs demonstrated the high reversibility of the charge storage mechanism, occurring at the active surface of GNP/CF electrodes.

The in-situ mechano-electrochemical testing results were further demonstrated, and figure S5 is the photograph of the experimental set-up. Different static loads were applied at midpoint of the specimens to induce different bending deflections. Results showed excellent in-situ mechano-electrochemical performance. There is no significant variation in electrochemical behaviour at various deflections until delamination occurs, as shown in Fig. 10(a). The low thickness and flexibility of the SSCs under flexural loads prevented immediate disruption of electrochemical pathways, contributing to this behaviour. Similar observations have been reported in several studies [48–50]. However, delamination at higher deflections has adversely affected for the long-term stability of the device, as shown in the Fig. 10(b). A gradual reduction in capacitance retention was observed with increasing deflection, reaching approximately 60 % at a deflection of 5 mm after 140 cycles.

3.6. *Proof of concept*

The developed double-cell SSC was utilized to light up a LED (Standard red, 5 mm, 2.3 V, 20 mA nominal current, 30 mA maximum current) to demonstrate SSC's use in a potential application. The double-cell device fabricated with CF/GNP 10 electrodes was used for this demonstration. First, the SSC was charged using a laboratory power supply of up to 5 V for 15 min, followed by measuring time durations that powered the LED ((Fig. 11(a)). The time duration while applying a three-point loading (at δ = 3 mm) was also measured (Fig. 11(b)). In both cases, the LED intensity decreased after 10 min, as shown in Fig. 11. The successful LED operation with and without loading confirmed the functionality of the developed structural supercapacitor.

In addition, a 300 mm × 300 mm large double-cell SSC was manufactured (figure S6) and compared the performance with 50 mm × 50 mm SSC. It demonstrated that energy storage can be increased proportionately to the structural supercapacitor size. Therefore, the proposed supercapacitor shows promising capabilities in energy storage

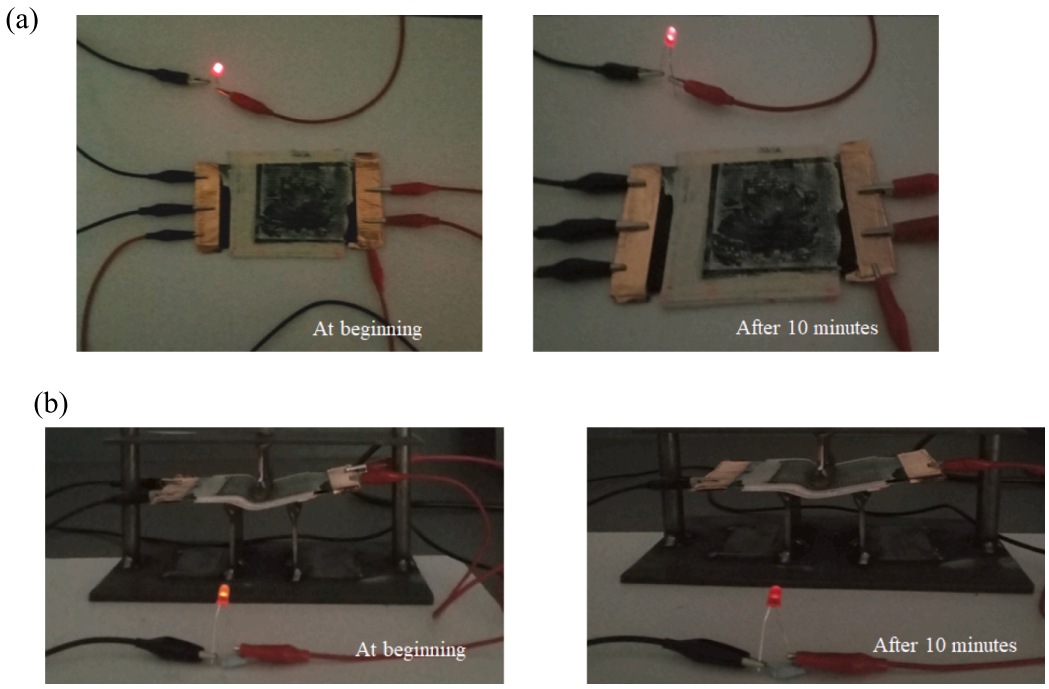

Fig. 11. Proof of concept of structural supercapacitor (50 mm × 50 mm) (a) without loading (b) with three-point loading.

applications.

4. Conclusion

A CF structural supercapacitor with high loading GNP has been developed and characterized. The developed CF structural supercapacitor has shown outstanding electromechanical performance. The GNP loading significantly enhanced the electrochemical and mechanical properties by increasing the surface area at the electrode/electrolyte interface. Additionally, GNP coating improved the surface wettability of CF electrodes with structural electrolytes, further improving the electrochemical performance. The optimized CF/GNP 20 double-cell structural supercapacitor demonstrates a remarkable specific capacitance of 123.5 mF g^{-1}, an energy density of 38.6 mWh kg^{-1}, and exceptional cycling stability up to 5000 cycles, exceeding some previously reported values. CF/GNP 10 double-cell structural supercapacitor has also shown the highest mechanical properties, with a tensile strength of 254.4 MPa and a bending strength of 48.9 MPa, demonstrating its ability to withstand significant structural load. In situ mechano-electrochemical tests revealed that SSC's electrochemical behaviour is unchanged under constant flexural load. Moreover, it maintained its electrochemical performance even after a mechanical failure, which underpins the robustness and suitability of the developed SSC for practical applications. Finally, a proof-of-concept was conducted to demonstrate the device's suitability for a practical application. Therefore, these findings can open up a new window of multifunctional composites and provide a new direction to furthering structural supercapacitor technology.

CRediT authorship contribution statement

Jayani Anurangi: Writing – original draft, Methodology, Formal analysis, Conceptualization. **Janitha Jeewantha:** Writing – review & editing, Methodology. **Madhubhashitha Herath:** Writing – review & editing, Supervision. **Dona T.L. Galhena:** Methodology. **Jayantha Epaarachchi:** Writing – review & editing, Supervision, Methodology, Conceptualization.

Funding

This research was supported by the AHEAD operation (Accelerate Higher Education Expansion and Development), a World Bank funded project in Sri Lanka.

Declaration of competing interest

The authors declare that they have no known competing financial interests or personal relationships that could have appeared to influence the work reported in this paper.

Appendix A. Supplementary material

Supplementary data to this article can be found online at https://doi.org/10.1016/j.compositesa.2024.108617.

Data availability

Data will be made available on request.

References

[1] Zenkert D, et al. Multifunctional carbon fibre composites using electrochemistry. Compos B Eng 2024;273:111240.
[2] Mutlu G, et al. Coating graphene nanoplatelets onto carbon fabric with controlled thickness for improved mechanical performance and EMI shielding effectiveness of carbon/epoxy composites. Eng Fract Mech 2023;284:109271.
[3] O'Brien DJ, et al. Effect of processing conditions and electrode characteristics on the electrical properties of structural composite capacitors. Compos A Appl Sci Manuf 2015;68:47–55.
[4] Anurangi J, et al. The use of fibre reinforced polymer composites for construction of structural supercapacitors: A review. Adv Compos Mater 2023:1–45.
[5] Javaid A, et al. Multifunctional structural supercapacitors based on polyaniline deposited carbon fiber reinforced epoxy composites. J Storage Mater 2021;33:102168.
[6] Adam TJ, et al. Multifunctional composites for future energy storage in aerospace structures. Energies 2018;11(2):335.
[7] Chu S, Majumdar A. Opportunities and challenges for a sustainable energy future. Nature 2012;488(7411):294–303.
[8] Qazi A, et al. Towards sustainable energy: A systematic review of renewable energy sources, technologies, and public opinions. IEEE Access 2019;7:63837–51.

[9] Shahbaz M, et al. Exploring the growth of sustainable energy technologies: A review. Sustainable Energy Technol Assess 2023;57:103157.
[10] Shang Y, et al. Excellent energy storage performance in polymer composites with insulating and polarized two-dimensional fillers. Compos A Appl Sci Manuf 2023;167:107429.
[11] Mapleback B, et al. Composite structural supercapacitors: High-performance carbon nanotube supercapacitors through ionic liquid localisation. Nanomaterials 2022;12(15):2558.
[12] Jiang J, et al. Influence of electrochemical oxidation of carbon fiber on the mechanical properties of carbon fiber/graphene oxide/epoxy composites. Compos A Appl Sci Manuf 2017;95:248–56.
[13] Liu Z, et al. Quantification of flexural fatigue life and 3D damage in carbon fibre reinforced polymer laminates. Compos A Appl Sci Manuf 2016;90:778–85.
[14] Forintos N, Czigany T. Multifunctional application of carbon fiber reinforced polymer composites: Electrical properties of the reinforcing carbon fibers–A short review. Compos B Eng 2019;162:331–43.
[15] Qiu B, et al. Fabrication of a high-temperature resistant and water-soluble sizing agent to significantly improve the interfacial properties of carbon fiber reinforced epoxy composites. Compos A Appl Sci Manuf 2024;185:108344.
[16] Sha Z, et al. Synergies of vertical graphene and manganese dioxide in enhancing the energy density of carbon fibre-based structural supercapacitors. Compos Sci Technol 2021;201:108568.
[17] Zhang M, et al. Surface modification of carbon fibers with hydrophilic Fe3O4 nanoparticles for nickel-based multifunctional composites. Appl Surf Sci 2020;509:145348.
[18] Sasikumar R, et al. Multifunctionality of MWCNT modified carbon fiber reinforced thermoplastic composite, and reclaiming composite in the pursuit of sustainable energy storage applications: An experimental and numerical analysis. Compos Sci Technol 2024;248:110468.
[19] Deka BK, et al. Multifunctional CuO nanowire embodied structural supercapacitor based on woven carbon fiber/ionic liquid–polyester resin. Compos A Appl Sci Manuf 2016;87:256–62.
[20] Asp LE, Greenhalgh ES. Structural power composites. Compos Sci Technol 2014;101:41–61.
[21] Zhou H, et al. Structural composite energy storage devices—A review. Mater Today Energy 2022;24:100924.
[22] Greenhalgh ES, et al. A critical review of structural supercapacitors and outlook on future research challenges. Compos Sci Technol 2023;235:109968.
[23] Javaid A, Irfan M. Multifunctional structural supercapacitors based on graphene nanoplatelets/carbon aerogel composite coated carbon fiber electrodes. Mater Res Express 2019;6(1):016310.
[24] Ganguly A, et al. Multifunctional structural supercapacitor based on urea-activated graphene nanoflakes directly grown on carbon fiber electrodes. ACS Appl Energy Mater 2020;3(5):4245–54.
[25] Shirshova N, et al. Structural composite supercapacitors. Compos A Appl Sci Manuf 2013;46:96–107.
[26] Zschiebsch W, et al. Multifunctionality analysis of structural supercapacitors— A review. Materials 2024;17(3):739.
[27] Ding Y, et al. High-performance multifunctional structural supercapacitors based on in situ and ex situ activated-carbon-coated carbon fiber electrodes. Energy Fuel 2022;36(4):2171–8.
[28] Hudak NS, Schlichting AD, Eisenbeiser K. Structural supercapacitors with enhanced performance using carbon nanotubes and polyaniline. J Electrochem Soc 2017;164(4):A691.
[29] Samsur R, et al. Fabrication of carbon nanotubes grown woven carbon fiber/epoxy composites and their electrical and mechanical properties. J Appl Phys 2013;113(21).
[30] Valkova M, et al. Predicting the mechanical behaviour of structural supercapacitor composites. Compos A Appl Sci Manuf 2022;156:106860.
[31] Subhani K, et al. Graphene aerogel modified carbon fiber reinforced composite structural supercapacitors. Compos Commun 2021;24:100663.
[32] Javaid A, et al. Improving the multifunctionality of structural supercapacitors by interleaving graphene nanoplatelets between carbon fibers and solid polymer electrolyte. J Compos Mater 2019;53(10):1401–9.
[33] Artigas-Arnaudas J, et al. Effect of electrode surface treatment on carbon fiber based structural supercapacitors: Electrochemical analysis, mechanical performance and proof-of-concept. J Storage Mater 2023;59:106599.
[34] Joseph A, et al. Recent advances in and perspectives on binder materials for supercapacitors–A review. Eur Polym J 2024;210:112941.
[35] Mahmood H, et al. Mechanical properties and strain monitoring of glass-epoxy composites with graphene-coated fibers. Compos A Appl Sci Manuf 2018;107:112–23.
[36] Zheng H, et al. Recent advances of interphases in carbon fiber-reinforced polymer composites: A review. Compos B Eng 2022;233:109639.
[37] Mishra K, Singh A. Effect of graphene nano-platelets coating on carbon fibers on the hygrothermal ageing driven degradation of carbon-fiber epoxy laminates. Compos B Eng 2024;269:111106.
[38] Cetinkaya T, Dryfe RAW. Electrical double layer supercapacitors based on graphene nanoplatelets electrodes in organic and aqueous electrolytes: Effect of binders and scalable performance. J Power Sources 2018;408:91–104.
[39] Zhu Z, et al. Effects of various binders on supercapacitor performances. Int J Electrochem Sci 2016;11(10):8270–9.
[40] Anurangi, J., Carbon Fibre Reinforced Bishphenol A Epoxy Composite Structures with energy storage capability in 11th Australasian Congress on Applied Mechanics. 2024.
[41] Anurangi J, et al. Electrochemical and structural performances of carbon and glass fiber-reinforced structural supercapacitor composite at elevated temperatures. Funct Compos Struct 2024;6(3):035004.
[42] *ASTM International 2022 D7334-08 Standard Practice for Surface Wettability of Coatings, Substrates and Pigments by Advancing Contact Angle Measurement (West Conshohocken, PA: ASTM International)*.
[43] *ASTM 2017 D3039/D3039M-17 Standard Test Method for Tensile Properties of Polymer Matrix Composite Materials (West Conshohocken, PA: ASTM International)*.
[44] *ASTM International 2017 D790-17 Standard Test Methods for Flexural Properties of Unreinforced and Reinforced Plastics and Electrical Insulating Materials (West Conshohocken, PA: ASTM International)*.
[45] Wu K-J, Young W-B, Young C. Structural supercapacitors: A mini-review of their fabrication, mechanical & electrochemical properties. J Storage Mater 2023;72:108358.
[46] *ASTM International 2022 D3171-22 Standard Test Methods for Constituent Content of Composite Materials (West Conshohocken, PA: ASTM International)*.
[47] Han Y, et al. Current collectors of carbon fiber reinforced polymer for stackable energy storage composites. Energy Storage Mater 2024;64:103070.
[48] Huang F, et al. Surface functionalization of electrodes and synthesis of dual-phase solid electrolytes for structural supercapacitors. ACS Appl Mater Interfaces 2022;14(27):30857–71.
[49] Zhou H, et al. A novel embedded all-solid-state composite structural supercapacitor based on activated carbon fiber electrode and carbon fiber reinforced polymer matrix. Chem Eng J 2023;454:140222.
[50] Liu X, et al. Achieving enhanced multifunctional performance for structural composite supercapacitors by reinforcing interfaces with polymer coating. J Colloid Interface Sci 2024;665:603–12.